

UC Davis

UC Davis Previously Published Works

Title

Comparison of cerebral blood flow measurement with [15O]-water positron emission tomography and arterial spin labeling magnetic resonance imaging: A systematic review

Permalink

<https://escholarship.org/uc/item/70v1t7c1>

Journal

Cerebrovascular and Brain Metabolism Reviews, 36(5)

ISSN

1040-8827

Authors

Fan, Audrey P
Jahanian, Hesamoddin
Holdsworth, Samantha J
[et al.](#)

Publication Date

2016-05-01

DOI

10.1177/0271678x16636393

Peer reviewed

Comparison of cerebral blood flow measurement with [^{15}O]-water positron emission tomography and arterial spin labeling magnetic resonance imaging: A systematic review

Audrey P Fan, Hesamoddin Jahanian, Samantha J Holdsworth and Greg Zaharchuk

Abstract

Noninvasive imaging of cerebral blood flow provides critical information to understand normal brain physiology as well as to identify and manage patients with neurological disorders. To date, the reference standard for cerebral blood flow measurements is considered to be positron emission tomography using injection of the [^{15}O]-water radiotracer. Although [^{15}O]-water has been used to study brain perfusion under normal and pathological conditions, it is not widely used in clinical settings due to the need for an on-site cyclotron, the invasive nature of arterial blood sampling, and experimental complexity. As an alternative, arterial spin labeling is a promising magnetic resonance imaging technique that magnetically labels arterial blood as it flows into the brain to map cerebral blood flow. As arterial spin labeling becomes more widely adopted in research and clinical settings, efforts have sought to standardize the method and validate its cerebral blood flow values against positron emission tomography-based cerebral blood flow measurements. The purpose of this work is to critically review studies that performed both [^{15}O]-water positron emission tomography and arterial spin labeling to measure brain perfusion, with the aim of better understanding the accuracy and reproducibility of arterial spin labeling relative to the positron emission tomography reference standard.

Keywords

Cerebral blood flow, perfusion imaging, positron emission tomography, arterial spin labeling, magnetic resonance imaging

Received 27 September 2015; Revised 19 January 2016; Accepted 4 February 2016

Introduction

The ability to noninvasively image cerebral blood flow (CBF) would enable improved identification and management of patients with many neurological disorders, including cerebrovascular and neurodegenerative diseases. Although various modalities exist to image perfusion,¹ clinicians still lack a robust, efficient method to quantify CBF in patients.

Currently, positron emission tomography (PET) with [^{15}O]-water is considered the reference standard for CBF measurements.^{2,3} In a typical experiment, [^{15}O]-water is injected into the patient and modeled as a freely diffusible tracer that enters into cerebral tissue but is not metabolized.⁴ Equilibrium is achieved within a few minutes, such that the integrated PET signal

reflects the perfusion status of the brain. [^{15}O]-water PET imaging usually requires a cyclotron at the imaging site due to the short half-life (~2 min) of oxygen-15. Patients must also undergo arterial cannulation to determine an arterial input function (AIF). These complexities significantly hinder the measurement of CBF in clinical settings.

As an alternative, arterial spin labeling (ASL) is a promising magnetic resonance imaging (MRI)

Department of Radiology, Stanford University, Stanford, CA, USA

Corresponding author:

Audrey Fan, Department of Radiology, Stanford University, 1201 Welch Road, Stanford, CA 94305, USA.

Email: audie@stanford.edu

technique that magnetically labels inflowing blood in feeding arteries proximal to the brain to map CBF. Separate “label” and “control” images (with no prior labeling of arterial blood) are acquired and the resulting ASL signal difference can be scaled to yield quantitative CBF values. The most common variants include pulsed ASL,^{5–7} which applies radiofrequency (RF) inversion pulses to a thick slab below the imaging slices; and pseudo-continuous ASL,^{8–10} which applies a train of RF pulses at a labeling plane below the imaging slices (for 1.5–2.5 s) to invert blood flowing through this plane. Similar to [¹⁵O]-water PET, the ASL technique treats water as a diffusible tracer, but the labeled blood is purely endogenous with a shorter half-life of approximately 2 s at 3 T. Because ASL is noninvasive, the control-tag experiment is typically repeated such that the final averaged perfusion signal provides higher signal-to-noise ratio (SNR) and spatial resolution CBF images compared with PET. A detailed comparison between the [¹⁵O]-water PET and ASL techniques is provided in Table 1. If ASL can replace PET for CBF measurements, clinicians and scientists would gain a valuable noninvasive tool to assess physiology during normal brain function and disease.

Table 1. Comparison of [¹⁵O]-water PET and ASL MRI methods to image brain perfusion.

Property	[¹⁵ O]-water PET	ASL MRI
Tracer	Radiolabeled water (injected)	Magnetically labeled water (endogenous)
Half-life of tracer	2 min	1650 ms (at 3 T) 1350 ms (at 1.5 T)
Ionizing radiation	Whole-body dose of 1.0–1.5 mSv	None
Spatial resolution	4–8 mm	1.8–4 mm
Acquisition time	3–10 min	3–6 min
Minimum time between scans	10 min	0 min
Reproducibility	5–10%	3–16%
Input function	Arterial blood sampling	Usually assumed; explicitly obtained in some ASL methods
Modeling	Kety–Schmidt (one-compartment) model	Microsphere model

^mASL: arterial spin labeling; MRI: magnetic resonance imaging; PET: positron emission tomography; CBF: cerebral blood flow; mSv: milliSievert.

Despite recent efforts to standardize ASL, the method currently lacks validation, especially in patients with abnormal vasculature. Although a number of studies have compared perfusion imaged by PET and MRI in the past 15 years, CBF scans from each modality were usually acquired in separate sessions, making it difficult to control for normal CBF variations with diet, hydration status, and diurnal cycles. Differences in findings may also reflect variability in the study design, including ASL acquisition parameters; availability of an AIF for the [¹⁵O]-water tracer; time elapsed between MRI and PET scans; and the study population. This review summarizes studies that have performed both PET and ASL CBF measurements and identifies technical requirements for future comparative studies that would more completely validate ASL for perfusion imaging.

Methodology for perfusion imaging in comparison studies

[¹⁵O]-water PET protocol

The [¹⁵O]-water PET method to quantify CBF requires the investigator to choose the radiotracer dose, how long to collect PET counts, how to temporally partition the PET counts, and how to determine the AIF. Each study performed a bolus injection of [¹⁵O]-water for 5–20 s. The total administered radioactivity primarily ranged between 15 mCi and 21.6 mCi,^{11–13} although one study relied on a larger dose of 40–46 mCi.¹⁴ Immediately after tracer administration, PET counts were collected over a time window of 3 min¹¹ up to 10 min.^{12,13,15} PET images were typically reconstructed with in-plane spatial resolution of 3 to 5 mm after filtering. A relative CBF image was available from these PET images through integration of PET counts from the first 1–2 min after arrival of the tracer bolus.^{16,17}

AIF. For quantitative studies, the AIF was measured by continuous, online sampling of arterial blood. These automated samplers typically draw arterial blood from a radial artery in the arm at a rate of 4–8.3 ml/min and measure the blood radioactivity through portable coincidence detectors (e.g. sodium iodide crystals) at high temporal resolution. A few groups additionally cross-calibrated the automated values against radioactivity in blood samples drawn manually at three time points (e.g. 5.5, 8, and 10 min) from the arm.^{12,13}

Because blood-based AIFs are usually estimated at the arm, the delay and dispersion of the tracer as it travels to the brain must be considered to accurately represent the [¹⁵O]-water input function. Time shifts between the blood samples and the PET scanner must also be corrected; some studies estimated this delay by

aligning the scanner count rates to the blood data,¹⁵ whereas others assumed a fixed time shift (e.g. 15 s) for each patient.¹⁸ The timing correction procedure for AIF estimation varied frequently across comparison studies. Previous simulation work has found that inaccuracies in the AIF timing can create 4–10% CBF overestimation for 2-s timing error, and up to 24% CBF overestimation for a 5-s timing error.²

Kinetic modeling and CBF map estimation. The Kety–Schmidt one-compartment model was adopted to quantify absolute CBF from [¹⁵O]-water uptake in brain tissue on the PET images and the AIF from blood samples. Three main implementations of this kinetic modeling were used across studies, including: (a) least-squares non-linear regression at each pixel;^{14,19,20} (b) the autoradiographic method, which creates a dictionary matching a ratio of time integrals (of the PET counts and AIF) to the underlying CBF;^{11,15} or (c) a basis function approach.^{12,13,21} The basis function approach assumes a physiologically plausible range of CBF and blood–brain partition coefficient parameters. A set of possible basis functions, i.e. the AIF convolved with an exponential term, are then created based on these parameters to linearize the one-compartment model for CBF estimation.²² In previous Monte Carlo simulations and human studies, non-linear regression and basis function approaches were consistent and gave accurate CBF estimates within 5% of the true simulated value for CBF settings of 100 ml/100 g/min or lower.²²

ASL MRI protocol

The ASL technique presents numerous acquisition and quantification choices that varied across studies, detailed in Table 2 for healthy volunteers and Table 3 for patients. All studies performed MRI scans on a 3 T systems (4 General Electric, 4 Philips, 3 Siemens), except for the study by Ye et al.,¹⁴ which used a 1.5 T MRI. For magnetic field strengths equal to or lower than 3 T, and for the range of echo times used in these studies, transverse relaxation effects on CBF are minimal. Figure 1 summarizes the impact of ASL protocol choices on CBF quantification.²⁵

Timing parameters. The ASL scans differed in the time elapsed between the labeling and image acquisition, during which tagged arterial blood travels to the imaging slice. In pulsed ASL, this delay is known as the inflow time (TI), and varied from 1400 ms¹⁵ to 1900 ms²³ across the studies summarized here. The post-label delay (PLD) parameter in pcASL experiments spanned a similar range from 1000 ms¹¹ to 1525 ms.¹³ In normal volunteers, we expect the ASL

signal to accurately reflect perfusion into the brain parenchyma if the TI or PLD time is greater than the arterial transit time (ATT). For healthy brains, TI and PLD values greater than ~1500 ms will allow sufficient time for tagged blood arrive at the imaging slice. The same ASL protocol was typically used in both patients and controls (Table 3). However, use of standard PLD or TI times may be problematic in patients if the ATT is altered due to disease-related abnormalities in the vessels. To avoid potential bias in CBF quantification, two patient studies^{18,21} adopted QUASAR pulsed ASL to acquire perfusion signals at multiple TI's, which should be less sensitive to ATT effects than single-TI methods.

The choice of TI and PLD parameters also changes the SNR of the ASL scan, in a complex manner that depends on the repetition time and the transit time of arterial blood. The PLD timing parameter (relative to the arterial arrival time and transit of tag into the tissue) and the chosen ASL labeling duration also lead to different arterial blood volume contributions to the ASL signal.²⁶ For this reason, the SNR of ASL scans differed across the studies we reviewed, and may influence the available statistical power to detect a relationship between PET and MRI CBF values from small cohorts.

T₁ relaxation. The accuracy of absolute CBF from ASL is heavily influenced by T_{1a}, the assumed T₁ relaxation value in arterial blood. This T_{1a} value depends on the hematocrit (Hct) level and may fluctuate dramatically with Hct in some populations, including neonates during their first few months of life.²⁷ Fast T₁ mapping techniques are not generally available on commercial MRI systems, and there is range of assumed T_{1a} values reported in the literature (1.4–2 s) that will affect perfusion quantification. For instance, given a true T_{1a} of 1650 ms and CBF of 50 ml/100 g/min, an incorrect assumed T_{1a} of 1400 ms would lead to a calculated CBF of 60 ml/100 g/min, i.e. an overestimation of 20%. One study chose to measure T_{1a} in each volunteer,¹³ and found mean values of 1695 ms for male subjects and 1779 ms for female subjects. Notably, other studies have assumed a wide range of T_{1a} values, ranging from 1250 ms¹⁴ to 1650 ms,^{18,19,21} which contributes to ASL CBF variability.

After the label arrives to the imaging slice, whether the subsequent signal is fit to a one-compartment or two-compartment ASL model affects the CBF quantification.²⁸ With a one-compartment model, the inverted label (flowing spins) continues to relax with T_{1a}, the value for arterial blood. In contrast, with a two-compartment model, the label transitions into the tissue environment; and decays faster with tissue T₁ relaxation of 1026 to 1200 ms in gray matter,^{29,30} or

Table 2. Acquisition and calibration parameters for ASL MRI in comparison studies of healthy volunteers.

Study	N	Sex (M:F)	Age (years)	ASL variant	TR/TE (ms)	Readout method	Label duration (ms)	Post-label delay (ms)	T ₁ , blood (ms)	Tag efficiency	Blood-brain partition
Ye et al. ¹⁴	12	5:7	38 ± 9	Continuous ASL	4700/17	Single-shot, 2D spin-echo spiral	3500	1100	1250	0.88	0.9
Qiu et al. ¹⁵	14	14:0	26 ± 7	Pulsed ASL with QUIPSS-II	2000/20	Gradient-echo EPI	–	T ₁₂ = 1400	1490	0.95	0.9
Xu et al. ¹⁶	19	4:4 6:5	31 (24–40) 61 (50–73)	pcASL	6000/21	3D fast spin-echo spiral	1500	1500	Measured ^a	0.85 × 0.75 (BS)	1.05
Henriksen et al. ¹⁹	17	8:9	24 (20–30)	Pulsed ASL with QUIPSS-II (QUASAR)	4000/22	Single-shot gradient echo EPI	–	Multiple T ₁ T ₁ = 40–3640 ΔT ₁ = 300	1650	0.91	0.9
Zhang et al. ¹¹	10	10:0	25 ± 3	pcASL	4150/14	Single-shot, 2D EPI	1400	1000	1493	0.86 ^a	0.9
Van Golen et al. ¹²	11	11:0	35 ± 14	pcASL	4300/9	3D fast spin-echo spiral	1500	1500	1400	0.8 × 0.75 (BS)	0.9
Kilroy et al. ¹⁷	6	5:1	68 ± 6	pcASL	4000/22	3D gradient and spin echo	1500	1500	1639	0.85 × 0.77 (BS)	0.9
Su et al. ²³	6	N/A	Young (ages not specified)	Pulsed ASL	3400 / 13	Single-shot, gradient-echo EPI	1200	T ₁₂ = 1900 ms	1664	0.95	0.9
Heijtel et al. ¹³	16	9:7	20–24	pcASL	3850/14	Single-shot, gradient-echo EPI	1650	1525	1695 ^a (male) 1779 ^a (female)	0.85 ^a	1.05

^aThese values were measured as part of the study and not assumed. ASL: arterial spin labeling; MRI: magnetic resonance imaging; TR: repetition time; TE: echo time; T₁: inflow time; pCASL: pseudocontinuous arterial spin labeling; EPI: echo planar imaging; BS: background suppression; QUIPSS-II: quantitative imaging of perfusion with single subtraction (Wong et al.⁶); QUASAR: quantitative STAR labeling of arterial regions (Petersen et al.²⁴).

Table 3. Acquisition and calibration parameters for ASL MRI in comparison studies of patients with various diseases.

Study	Patient cohort	N	Sex (M:F)	Age (years)	ASL variant	TR/TE (ms)	Readout method	Label duration (ms)	Post-label delay (ms)	T1, blood (ms)	Tag efficiency	Blood-brain partition
Xu et al. ¹⁶	Alzheimer's disease and mild cognitive impairment	3	N/A	61 (50-73)	pcASL	6000/21	Fast 3D spin-echo spiral	1500	1500	Measured ^a	0.85×0.75	1.05
Bokkers et al. ²¹	Internal carotid artery occlusion	14	9:5	63 ± 14	Pulsed ASL (QUASAR)	4000/23	Single-shot gradient echo EPI	-	Multiple TI 200-2600 Δ TI=200	1650	-	0.9
Kamano et al. ¹⁸	Chronic cerebral arterial steno-occlusive disease	16	11:5	61 ± 16	Pulsed ASL (QUASAR)	4000/22	Single-shot gradient echo EPI	-	Multiple TI 50-2650 Δ TI=200	1650	0.95	0.98 (gray matter) 0.82 (white matter)
Goetti et al. ²⁰	Moya-Moya disease	13	5:8	10 ± 7	pcASL	5500/25	3D fast spin-echo spiral	1500	1500	1600	0.95×0.75 (BS)	0.9
Van Golen et al. ¹²	Type I diabetes	20	20:0	36 ± 10	pcASL	4300/9	3D fast spin-echo spiral	1500	1500	1400	0.8×0.75 (BS)	0.9
Kilroy et al. ¹⁷	Alzheimer's disease and mild cognitive impairment	7	4:3	68 ± 6	pcASL	4000/22	3D gradient and spin echo	1500	1500	1639	0.85×0.77 (BS)	0.9

^aThese values were measured as part of the study and not assumed. ASL: arterial spin labeling; MRI: magnetic resonance imaging; TR: repetition time; TE: echo time; pcASL: pseudocontinuous arterial spin labeling; EPI: echo planar imaging; BS: background suppression; QUASAR: quantitative STAR labeling of arterial regions (Peterson et al.²⁴).

with an even lower T_1 of 600 ms in white matter.²⁹ As a result of this T_1 transition, the same ASL signal modeled by the two-compartment model provides higher quantitative CBF than the one-compartment model for typical values of tissue T_1 . Of the nine studies in Table 2, five used the one-compartment model, three used the two-compartment model, and one used a “model-free” approach to characterize the multi-delay ASL time course. The more physiologically accurate two-compartment model likely provides CBF values closer to PET than the one-compartment model, although a careful comparison has not been performed.

Additional technical considerations. In ASL, moving labeled spins that remain in large arteries may contribute to a focal CBF overestimation. One approach to address this contamination is to apply flow crusher gradients, e.g. symmetric gradient pulses before and after each RF inversion (labeling) pulse, to dephase moving spins and suppress intravascular flow signal. Among the studies listed in Tables 2 and 3, half of the investigations (6/12) applied crusher gradients in their ASL acquisition. While crusher gradients are important to avoid focal CBF overestimation due to large vessels, they may reduce SNR and are thus ill-suited to low-SNR applications such as multi-delay ASL. It is also important to remember that crusher gradients remove some of the labeled water; if this effect is not accounted for, one would expect a global CBF underestimation.

To a lesser extent, the assumed labeling efficiency (α) of the ASL magnetic tag also affects CBF. This α parameter corrects for incomplete tagging of the arterial blood due to off-resonance or excitation field inhomogeneity at the labeling position,^{31,32} and differs between ASL labeling types. In the studies we reviewed, α was assumed to be greater than 0.9 for pulsed labeling strategies, whereas α was assumed to be between 0.8 and 0.85 for most pseudo-continuous labeling strategies. Two studies directly measured labeling efficiency in volunteers as part of the pcASL protocol,^{11,13} through use of reference phase-contrast MRI scans to assess total brain blood flow. Studies that adopted MRI background suppression pulses typically included an additional attenuation factor of 0.75 to the assumed value of α .^{12,16,17,20}

CBF measurements by PET and ASL in healthy volunteers

Quantitative CBF findings by PET and MRI

To evaluate comparisons of quantitative CBF, articles were selected based on a PubMed search of the terms “Arterial spin labeling MRI” and “O-15 PET.” The

search was limited to studies in the past 15 years that performed absolute CBF measurements with PET and ASL in healthy volunteers. We identified seven quantitative studies that satisfied the search criteria.^{11–15,19,23} Some of these studies have also been described in a recent review article from Zhang et al. that focused on ASL comparisons with [¹⁵O]-water PET, [¹⁸F]-FDG PET, perfusion SPECT, and contrast perfusion MRI in a range of diseases, including Alzheimer’s disease.³³

Figure 2 depicts the mean absolute CBF for the whole brain and in the gray matter imaged by PET and MRI for these studies. In most (6/7) of these reports, global ASL CBF values were within 15% of the PET CBF values. Across the studies, the weighted-average global CBF was 44.2 ± 9 ml/100 g/min by PET and 41.5 ± 9 ml/100 g/min by ASL. As expected, gray matter CBF values were higher than the whole-brain values; gray matter CBF was 53.9 ± 11 ml/100 g/min by PET and 54.1 ± 10 ml/100 g/min by ASL.

In Figure 2, the studies that used pcASL imaging generally overestimated CBF relative to the PET reference standard. For example, pcASL showed as much as 20% global overestimation of whole-brain CBF¹¹; and 7% overestimation of gray matter CBF relative to PET.¹³ On the other hand, pulsed ASL tended to underestimate CBF with MRI by approximately 12% compared with PET.^{19,23,34} The source of these trends is unclear, since other ASL studies directly comparing pulsed to pseudo-continuous ASL did not observe a bias between the labeling strategies.^{35–37} One contributing factor is that the PLD times used in pcASL studies were generally shorter than TI times adopted in pulsed ASL studies (Table 2). For PLD delay times much shorter than 1500 ms, gray matter CBF values may be overestimated due to contamination from residual labeled blood in arteries that is misattributed to the tissue.³⁸ This potential overestimation is consistent with the trends seen in Figure 2. To fully understand the impact of different labeling strategies requires additional direct comparisons between pulsed ASL and pcASL in future work.

We also corrected ASL measurements to use consensus values of T_{1a} (1650 ms); tag efficiency (0.85 for pcASL, 0.9 for pulsed ASL); and blood–brain partition coefficient (0.9 ml/g).³⁹ In 2/7 of the quantitative studies, we recalculated the CBF measurement to use the one-compartment instead of two-compartment ASL model. These corrections did not improve the overall consistency of PET and ASL methods (Figure 2, blue crosses). However, the correction lowered the mean ASL CBF values across studies for whole-brain (corrected CBF = 36.5 ml/100 g/min) and gray matter values (corrected CBF = 47.5 ml/100 g/min). We note that the studies by Ye et al.¹⁴ and Van Golen et al.¹² showed

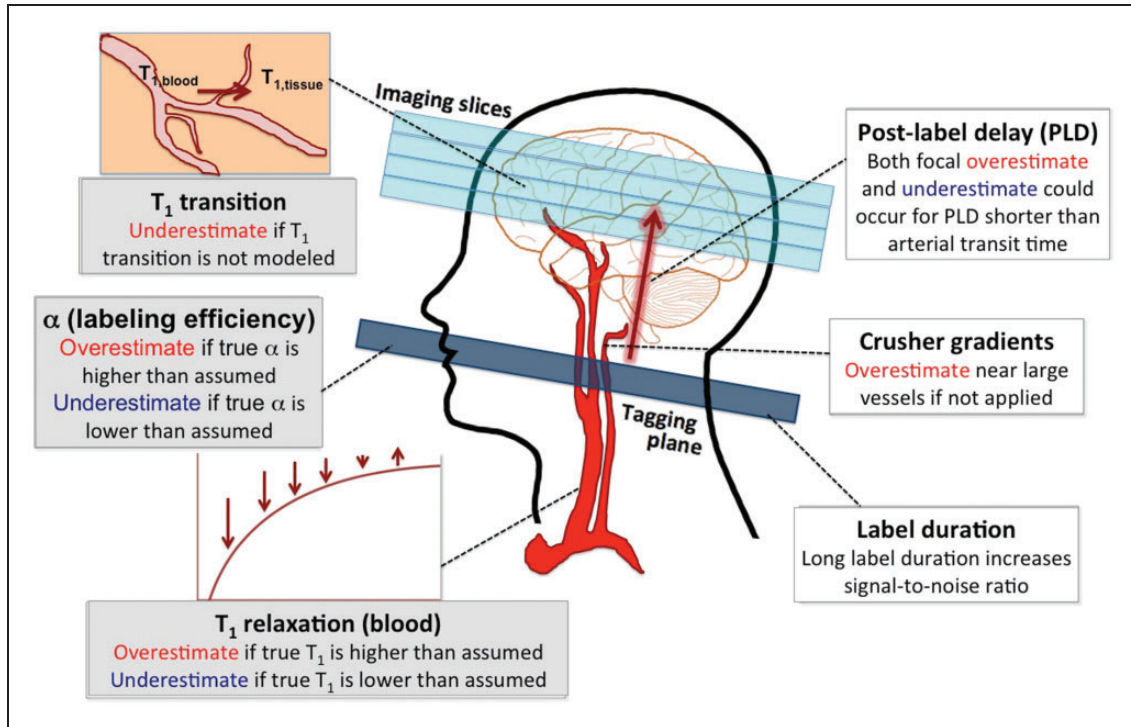


Figure 1. Schematic of CBF quantification challenges with ASL MRI. ASL issues related to assumed constants are shown on the left (gray boxes), including the T_1 transition of label from blood to tissue, the labeling efficiency α , and the T_1 relaxation of arterial blood. ASL issues related to imaging parameters selected by the user are shown on the right (white boxes), including the post-label delay, use of crusher gradients, and labeling duration. ASL: arterial spin labeling; MRI: magnetic resonance imaging.

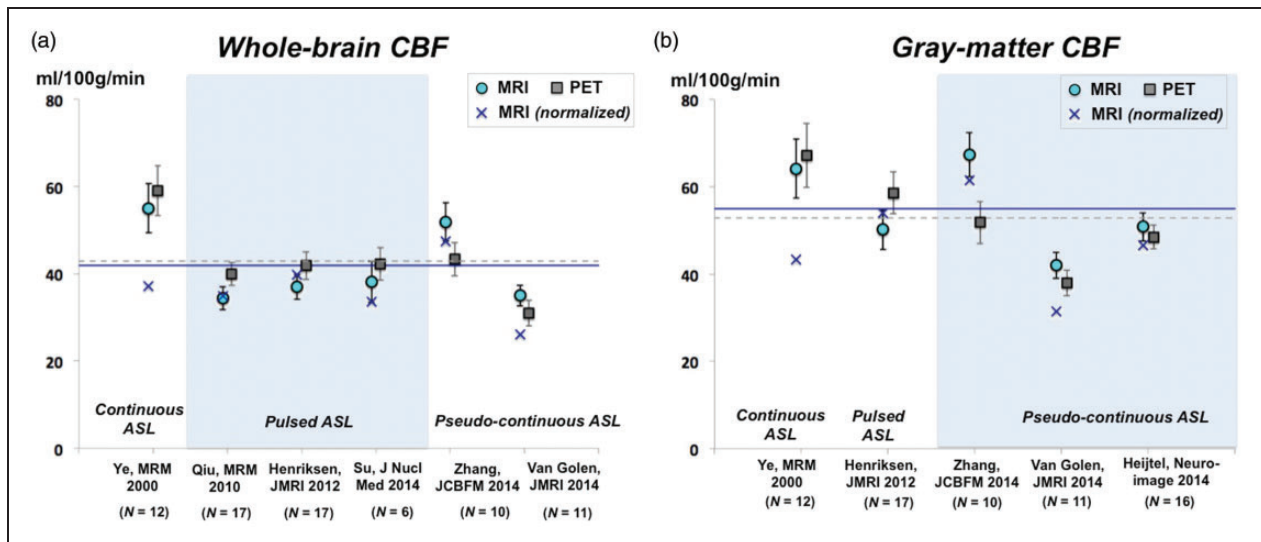


Figure 2. Mean baseline cerebral blood flow (ml/100 g/min) measured by ASL MRI and $[^{15}\text{O}]$ -water PET in comparative studies across the (a) whole brain and (b) the gray matter. Studies are grouped based on the variant of ASL used for comparison against the PET gold standard. Error bars are estimated 95% confidence intervals that account for the sample size of each study. The solid blue line represents the mean PET CBF values and the dotted gray line represents the mean ASL CBF values across the studies. For each study, the MRI values were also normalized (blue crosses) using the one-compartment model with standardized values for assumed ASL constants in Alsop et al.³⁹ ASL: arterial spin labeling; MRI: magnetic resonance imaging; PET: positron emission tomography; CBF: cerebral blood flow.

dramatically lower ASL CBF after the correction, most likely because the original assumed T_{1a} values (1250 ms and 1400 ms, respectively) were much lower than the consensus value of 1650 ms.

Regional aspects of CBF comparisons

In regional and voxel-wise analyses, the CBF agreement between PET and ASL often varied spatially across the brain. These spatial variations can inform users about technical considerations related to the ASL method. For instance, Ye et al.¹⁴ observed that absolute CBF within a central cortical strip region of interest (ROI) was not different by continuous ASL and by PET; however, MRI underestimated absolute CBF in a central white matter ROI by 30% compared with PET. ASL is difficult to implement in white matter because of its longer transit time, which artificially reduces the achievable ASL signal.⁴⁰ In general, ASL in white matter is also known to have poor reliability and SNR because its blood flow is 2–3.6 times lower than that of gray matter.⁴¹ Other studies compared

regional CBF within smaller ROIs based on a brain atlas and found differences in specific ROIs due to high measurement variance or intrinsic regional tissue properties that affect the ASL signal.^{11,12}

In recent literature, voxel-based morphometry has been performed to spatially align images into a common stereotactic space, enabling averaging across subjects.⁴² With voxel-wise statistical tests, previous groups have detected areas of higher CBF by pcASL (deep cortical tissues including the cingulate cortex); and areas of lower CBF by pcASL (basal ganglia) compared with PET.^{12,13} These areas of systematic over- or underestimation of CBF may elucidate potential sources of bias in the ASL technique. For instance, underestimation of CBF in the prefrontal areas¹³ likely reflects susceptibility-induced distortions near the sinuses that manifest on echo-planar readout ASL images (Figure 3); such a finding would not be expected with newer 3D spin echo readout strategies. This spatial mapping approach also facilitates visualization of the effect of ASL technical improvements, such as the addition of MRI crusher gradients to the pcASL sequence

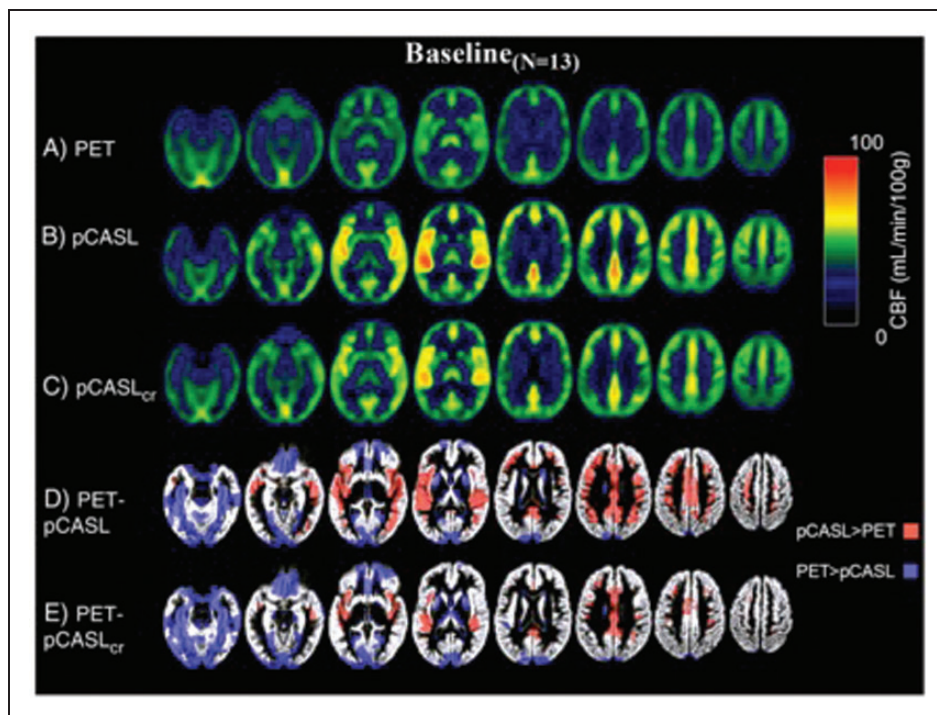


Figure 3. Mean CBF maps across 16 healthy volunteers measured by (a) [^{15}O]-water PET, (b) pseudo-continuous ASL (pcASL), and (c) pcASL with MRI crusher gradients. Voxel-wise statistical parametric testing ($P < 0.001$) reveals areas in which pcASL overestimates (red) or underestimates (blue) quantitative CBF relative to PET (d,e). This analysis revealed systematic overestimation of pcASL CBF in deep cortical tissues and systematic underestimation in the prefrontal area, basal nuclei, and near the sagittal sinus. The difference between rows (d) and (e) reveal that additional crusher gradients in the pcASL MRI sequence reduces the areas of overestimation. Source: reproduced with permission from Elsevier, 2014.¹³

ASL: arterial spin labeling; MRI: magnetic resonance imaging; PET: positron emission tomography; CBF: cerebral blood flow.

(Figure 3(d) to (e)). Interestingly, the use of crushers reduced the areas of CBF overestimation by ASL (due to contamination from macrovascular compartments and inappropriate choice of PLD), but did not improve areas of CBF underestimation.

Partial volume effects on PET and MRI

Both ASL and PET experience CBF underestimation in gray matter due to partial volume effects. ASL CBF maps have higher spatial resolution (3–3.4 mm) than PET (6.5–7 mm),^{13,21} but are still prone to partial voluming within the thin and convoluted cortex (2–3 mm in thickness). Since ASL and PET each have vastly different spatial resolutions, regional CBF biases between techniques may arise due to different effects of partial volume on each modality. Whether the CBF maps are smoothed to the same resolution before comparison,¹² or interpolated to a common space^{15,16,19} versus the native perfusion space,²¹ may also influence quantitative comparisons. These registration procedures varied widely in software and methodology across the studies reviewed here.

In future validation studies, differences in partial volume effects should be considered for CBF assessment in diseases that may result in tissue volume changes. For instance, a PET study of healthy aging found a significant inverse correlation between age and cortical CBF, but this trend was not present after adjusting for partial voluming.⁴³ Inappropriate treatment of partial volume effects could create different patient CBF results by different techniques. Partial volume corrections that have been proposed for PET^{44,45} and ASL^{46,47} often model each voxel's signal as the weighted contribution of different tissue types,

either statically or dynamically within the perfusion kinetic model. These corrections may need to be performed differently for each modality to mitigate CBF biases due to limited spatial resolution.

Time elapsed between PET and MRI measurements of CBF

For the comparison studies summarized in this article, PET and MRI CBF measurements were typically made in separate sessions. The time elapsed between the CBF scans ranged from hours,^{16,17} a week,^{13,21} multiple weeks,^{12,20} or up to 3 months.¹⁹ Because the two scans were performed on separate machines at different times, discrepancies could reflect CBF fluctuations over time, which are hard to disentangle from differences in the underlying methods. Previous scan–rescan tests by [¹⁵O]-water PET have found a 10% variation in gray matter and 8% variation in white matter for an interval of 2 days.⁴⁸ ASL reproducibility scans revealed similar 14% variation for an interval of a week, and 6% variation even for measurements repeated within an hour.⁴⁹

To account for normal diurnal variations in CBF,^{50,51} perfusion scans should be performed at the same time of day for optimal reproducibility. Variations with the menstrual cycle⁵² should also be considered for female subjects. Furthermore, diet-related effects on perfusion, most notably CBF reduction due to caffeine intake,^{53,54} can be large and need to be minimized. These factors are difficult to control, especially for retrospective analyses,^{18,20} although some studies required volunteers not to ingest caffeine or nicotine in the hours before the imaging study.^{11,16,17,19} Table 4 summarizes the control of various physiological variables; half of the comparison studies controlled for caffeine intake, but fewer

Table 4. Control of physiological variables in comparison studies of perfusion imaging.

Study	Design	Time of day	Caffeine intake	Fasting
Ye et al. ¹⁴	Prospective	No	No	No
Qiu et al. ¹⁵	Prospective	No	No	No
Xu et al. ¹⁶	Prospective	No	Yes (3 h before exam)	No
Bokkers et al. ²¹	Prospective	No	No	No
Henriksen et al. ¹⁹	Prospective	No	Yes (8 h before exam)	No
Kamano et al. ¹⁸	Retrospective	No	No	No
Zhang et al. ¹¹	Prospective	Simultaneous	Simultaneous	Simultaneous
Goetti et al. ²⁰	Retrospective	No	No	No
Van Golen et al. ¹²	Prospective	Yes	Yes (10 h before exam)	Yes (10 h before exam)
Kilroy et al. ¹⁷	Prospective	No	Yes (3 h before exam)	No
Su et al. ²³	Prospective	Simultaneous	Simultaneous	Simultaneous
Heijtel et al. ¹³	Prospective	No	No	No

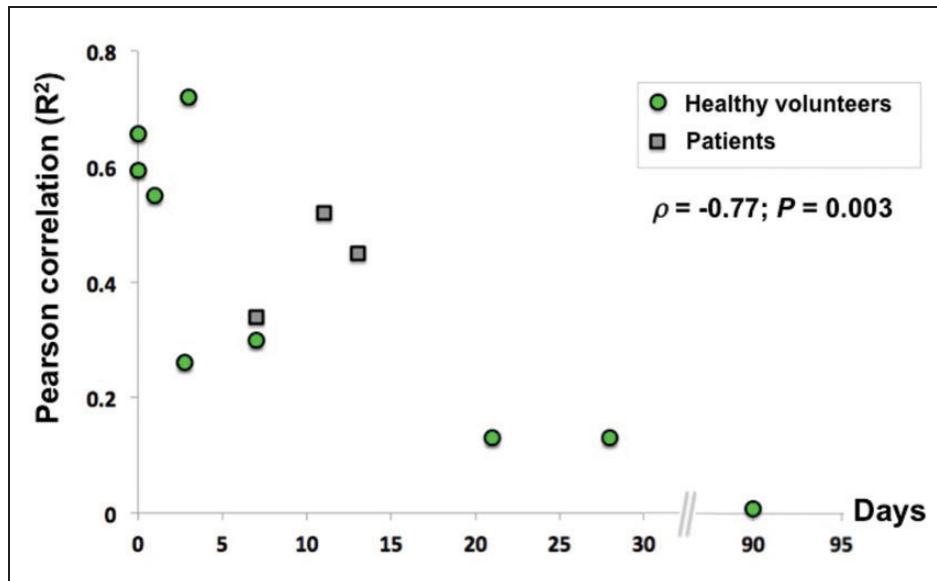


Figure 4. Pearson correlation coefficient (R^2) between [^{15}O]-water PET and ASL MRI perfusion measurements reported in comparison studies, plotted against the time elapsed between the PET and MRI scans. Correlations are presented for both absolute and relative CBF metrics, as well as for healthy volunteers (green) and patient populations (gray). Across studies, Spearman rank correlation revealed an inverse relationship between the reported R^2 values and the elapsed time ($\rho = -0.77$, $P = 0.003$). ASL: arterial spin labeling; MRI: magnetic resonance imaging; PET: positron emission tomography; CBF: cerebral blood flow.

controlled for the time of day or required volunteers to fast before the imaging exam.

While most of these factors could not be assessed for the studies, we examined whether the agreement between PET and MRI related to the time interval between the scans. Figure 4 plots the Pearson correlation coefficient between PET and MRI for each study, including relative and quantitative studies, against the time elapsed between imaging sessions. Across studies, Spearman rank correlation ($\rho = -0.77$, $P = 0.003$) revealed an inverse relationship between the reported R^2 values and the elapsed time. Thus, the consistency between PET and MRI CBF tended to be higher for measurements that are closely spaced in time; future comparison studies should aim to reduce this elapsed time as much as possible.

Simultaneous PET-MRI: Blessing or curse for comparing quantitative CBF?

New hybrid PET-MRI systems are an ideal validation tool that allows for simultaneous observations of CBF, thereby ensuring that the same physiologic perfusion state of the brain is imaged by each modality. Although sequential scans with minimal inter-scan delay may be sufficient for validation, the logistical challenge of coordinating multiple exams led to extended delays between the PET and MRI exams in many of the studies we reviewed. Because only one imaging session is required to obtain information by

both modalities, the hybrid scanner greatly facilitates the logistics of validation.

Two studies have directly compared ASL to concurrent PET with a hybrid system.^{11,23} Zhang et al. used a prototype Siemens BrainPET insert, comprised of MRI-compatible PET detectors, to acquire simultaneous PET and MRI.¹¹ By avoiding physiological variations between different sessions, this work achieved high correlation between PET and pcASL for mean values across the gray matter ($R = 0.80$) and white matter ($R = 0.94$). However, regional CBF in the gray matter was still 29% higher by pcASL relative to PET.¹¹ This finding suggests methodological biases unrelated to CBF physiologic variations that preferentially affects the gray matter in their ASL implementation. While the ASL measurement bias for mean white matter CBF was lower (12%), voxelwise variations and noise in the white matter were still greater. In a separate study, high correlation ($R = 0.77$) was also observed between simultaneous PET and pulsed ASL scans for whole-brain CBF values.²³

While the PET-MRI offers truly simultaneous imaging of CBF by two modalities, it also brings unique technical challenges. A key concern is the lack of CT data for attenuation correction of PET images. Zhang et al. relied on a template-based attenuation correction based on the MRI structural scan acquired in each volunteer and knowledge of the attenuation properties and position of the imaging coils. These techniques are still under development and may contribute artifacts on the

reference PET images. Nonetheless, the meta-analysis in Figure 4 and promising initial studies suggest that upcoming PET-MRI systems can facilitate ASL validation without errors related to different perfusion states at different scan times.

Perfusion measurements by PET and MRI in patients with neurological and metabolic diseases

For perfusion imaging to be clinically useful, reliable CBF measurements must be available in patients with altered cerebrovascular physiology. These patients may exhibit global changes in CBF with age⁵⁵ or neurodegenerative disease;^{56,57} or exhibit local CBF changes as in arterial occlusive disorders.^{58–60} Even in cases where absolute tissue perfusion is not affected by disease, arterial transit time (ATT) may be prolonged if blood is forced to flow through collateral vessel pathways.⁶¹

Because the [¹⁵O]-water PET method relies on an exogenous injected tracer and computes CBF from the time integral of PET counts in local tissue, it is sensitive across multiple CBF levels and is robust to a wide range of ATTs. Thus, the same PET protocol for CBF assessment may be used for healthy persons and patients. On the other hand, ASL endogenously labels arterial blood and waits a pre-determined delay time (1.5 to 4s) for the tag to arrive at the imaging slice. In patients with cerebrovascular disease, prolonged ATTs may lead to inaccurate CBF values if post-label delay is not adjusted accordingly. For instance, prolonged ATTs could lead to focal underestimation of CBF if the tag has not arrived to the acquisition plane at the time of imaging; or lead to regional CBF inaccuracy if residual labeled blood remains in slow-flowing vessels. ASL sequences thus must be tailored for CBF assessment in certain patient cohorts.

Cerebrovascular disorders

Goetti et al.²⁰ applied a standard pcASL sequence with a single PLD time of 1500ms in children and young adults with Moyamoya disease to compare with PET. Visual evaluation by clinicians identified regions of impaired flow (40% of the segmented vascular territories) related to disease; these qualitative findings were largely concordant between the PET and MRI scans. However, in quantitative analysis, measured CBF values were lower on ASL compared with PET, especially in areas that with visibly reduced perfusion.²⁰ The authors suggested that this was partly due to long transit times through collateral pathways in Moyamoya patients. Because of long ATTs, the labeled blood may not have fully arrived at the imaging plane, leading to

signal loss and artificially low CBF values by ASL. While Goetti et al. could have used a longer PLD (i.e. 2s or longer) to ensure arrival of the label, this would have led to more severe T₁ decay of the signal and reduced SNR. With a single PLD time, the tradeoff is as follows: enough time must elapse for the tag to reach the imaging slice including through collateral pathways (i.e. the PLD should be longer than the ATT); however, imaging must also occur before substantial label decay occurs.

To avoid problems due to long ATTs in single-delay ASL, two studies instead used multi-delay time ASL techniques for patients with cerebrovascular disease. With multiple TI's or PLD's, multi-delay ASL enables ATT estimation and can correct CBF based on the ATT.⁶² Bokkers et al. used TI times between 200 and 2600ms in patients with symptomatic internal carotid artery occlusion.²¹ Kamano et al. used a similar range of TI times between 50 and 2650ms in patients with chronic cerebral arterial steno-occlusive disease.^{18,24} The perfusion signal was modeled over the multiple delay times to quantify CBF maps,^{24,63} and both studies detected strong correlations between PET and MRI CBF values.^{18,21} As this modeling does not assume a fixed time of tag arrival, it is expected to provide more robust CBF estimates in the presence of long ATTs relative to single PLD methods. This advantage is illustrated in a patient with unilateral Moyamoya disease in Figure 5. On the multi-delay pcASL scans, the symptomatic hemisphere showed preserved perfusion but long ATTs. These elongated ATTs led to artificially low ASL signal at shorter PLD times (e.g. 700 or 1300ms), which would manifest as CBF underestimation with a single-PLD approach if the selected PLD time is too short relative to the ATTs.

However, even with the use of multi-delay ASL, inconsistencies remained between PET and MRI in patients with cerebrovascular disorders. For instance, Bokkers et al. calculated the ratio between perfusion of the symptomatic hemisphere to the contralateral hemisphere.²¹ ASL overestimated the difference between the symptomatic and contralateral hemispheres in the gray matter near the middle cerebral artery, but not in areas near the anterior or posterior cerebral arteries. The authors hypothesized that the particular anatomy of the MCA vasculature led to high residual intravascular ASL signal, which had not yet diffused into the local tissue. This observation motivates future ASL technical development in problematic areas of slow flow in patients.

Healthy aging and neurodegenerative diseases

Perfusion imaging provides insight into physiological changes during healthy aging and neurodegenerative

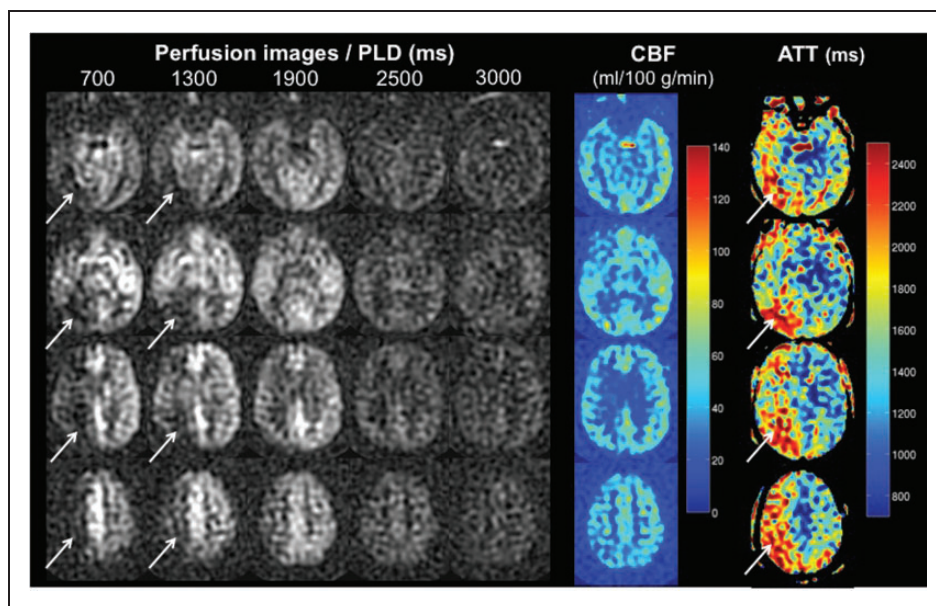


Figure 5. Multi-delay ASL images from a patient with unilateral Moyamoya disease of the right hemisphere. Perfusion images are shown for different PLD times; note that signal decays with increasing PLD, as expected. Arrows indicate areas of low ASL signal on images collected with short PLD times. The multi-delay ASL scans revealed long ATT in these same regions of the occluded hemisphere, suggesting that for PLD = 700 or 1300 ms, not enough time has elapsed for the label to travel through collateral vessels and fully arrive to the imaging volume. If a single-delay ASL technique had been used, inappropriate choice of PLD may have led to CBF underestimation in the symptomatic hemisphere. However, multi-delay ASL imaging indicates that perfusion is preserved in the symptomatic relative to the normal-appearing hemisphere (middle panel).
ASL: arterial spin labeling; CBF: cerebral blood flow. PLD: post-label delay; ATT: arterial transit time.

disorders. Some imaging studies have found that gray matter CBF declines with age,^{64,65} whereas others have not observed strong age-related trends.^{43,66} Perfusion deficits have also been observed in Alzheimer's disease (AD) and mild cognitive impairment (MCI),^{67–69} although typically in studies with small sample sizes. These populations present unique challenges for ASL measurements, due to the reduced image SNR that accompanies lower CBF, and require careful comparison against PET.

To address this need, two studies performed both PET and ASL in elderly subjects and in patients with AD and MCI.^{16,17} Each study found significant associations between PET and ASL CBF, with Pearson correlations greater than 0.5 across all ROIs. Despite technical challenges with use of ASL in elderly patients, both studies also reported high test–retest intraclass coefficient correlations (ICC) of 0.93¹⁶ and 0.78¹⁷ between the two modalities in the gray matter. In fact, Xu et al. observed higher gray matter SNR with ASL (8.86 ± 2) compared with PET (6.4 ± 1) in their elderly cohort. ICC values in the white matter also of good quality, although PET offered better SNR than ASL in the white matter. This work reaffirms the potential of ASL to detect more subtle CBF changes, even in these challenging populations.

Although neither study had sufficient sample size to assess disease-related trends, Xu et al. did see a decrease in the ratio of CBF in gray matter to white matter with age.¹⁶ These findings must be interpreted carefully because they are based on single-delay time ASL scans. If the selected single PLD time is not long enough to allow complete delivery of the label to the tissue, ATT changes related to disease or age may alter the apparent CBF. Since ATT in elderly patients is likely longer than younger people,^{65,70} the effect of different ATTs could act a potential confounder. Future work in elderly individuals could investigate multiple-delay time ASL scans that are more robust to variable ATTs.

Metabolic disorders

Patients who suffer from metabolic disorders including diabetes may also benefit from imaging of brain perfusion. In these patients, large oscillations in blood glucose and insulin levels may damage the vascular wall⁷¹ and directly affect CBF to the peripheral tissues;^{72,73} or they may create increases in neuronal metabolic activity that manifest as elevated CBF in glucose-sensing brain networks.^{74,75} Early [¹⁵O]-water PET studies have sought to characterize brain areas of increased CBF in diabetic persons,^{76,77} but have

been limited in scope by the complexity of PET experiments.

Van Golen et al. investigated whether ASL is a suitable replacement for PET to study baseline CBF in healthy adults and patients with type 1 diabetes.¹² ASL overestimated CBF relative to PET in both the gray and white matter, particularly in the anterior and posterior cingulate cortices ($P < 0.001$). The authors suggested potential biases due to the assumed T_1 relaxation value of arterial blood and blood-brain partition coefficient values used in the ASL measurements. Given the small cohort, van Golen et al. did not find any disease-driven difference in resting CBF between patients and controls, but did reveal a consistent overestimation of CBF by ASL, including in the diabetic patients.

Arbeláez et al. instead focused on the CBF response to a metabolic challenge in healthy volunteers.⁷⁷ Participants were imaged by PET and MRI during periods of high and low blood glucose levels created by variable infusions of glucose. Both PET and pulsed ASL identified similar focal increases in CBF within the thalamus, medial prefrontal cortex, and globus pallidus during hypoglycemia compared with the euglycemia ($P < 0.05$). This study highlights the potential of ASL to measure CBF changes in various metabolic states, and may be applied in future work to detect disease-driven differences in the CBF response to metabolic challenges.

Relative CBF measurements by PET and MRI: Are relative metrics sufficient?

In some clinical applications, patient evaluation focuses on localized perfusion abnormalities, and internal calibration of the affected (ipsilateral) versus contralateral hemispheres of the brain may be more important than absolute perfusion. In these scenarios, relative CBF provides useful information about symptomatic brain regions compared with normal-appearing tissue^{16,17,20} and may even outperform current quantitative metrics to predict infarct growth.^{78,79} For these applications, the reproducibility, sensitivity, and diagnostic ability of relative metrics (e.g. CBF ratios between infarct, penumbra that infarcts, and penumbra that recovers in acute stroke) are also important to consider.⁸⁰

Several studies have compared relative perfusion measurements at baseline^{16–18,20} or during evoked CBF changes with a visual task.^{81,82} One rationale to use relative metrics for validation is to avoid arterial blood sampling to determine the AIF, which is necessary to quantify absolute CBF maps from the [¹⁵O]-water PET experiment. Arterial sampling requires cannulation of an artery and adds discomfort that is undesirable in many situations, particularly in

specialized populations such as older adults and young children. PET CBF quantification without arterial sampling is challenging, because the assumed AIF and tracer kinetics may not apply to all individuals.

To avoid arterial sampling, Xu et al. created PET CBF images by first integrating the initial 60 s of tracer uptake and then normalizing to mean whole brain perfusion.¹⁶ Similarly, Kilroy et al. scaled all PET CBF maps to a global mean of 50 ml/100 g/min.¹⁷ Both studies found good correlation between relative CBF by PET and absolute CBF by pcASL MRI, including in older adults over 55 years of age. In contrast, Goetti et al.²⁰ first calculated absolute PET CBF images via kinetic modeling with a standardized, population-based AIF in children and young adults with Moyamoya disease. Although mean absolute CBF measured by pcASL was only slightly lower than CBF by PET, there was no association between the PET and MRI values across subjects. In further analysis, the authors instead computed relative PET CBF maps by normalizing to the cerebellar CBF. Only the relative CBF maps showed good agreement between the two modalities ($R = 0.67$, $P < 0.001$).

Even when blood samples were available, some investigators opted to compare relative CBF metrics. Kamano et al. collected arterial blood samples in patients with chronic cerebral arterial occlusion and found good agreement between absolute CBF by PET and absolute CBF by MRI ($R = 0.52$, $P < 0.0001$).¹⁸ Normalization of the values to the mean across ROIs further improved this correlation for relative perfusion ($R = 0.69$, $P < 0.0001$). The authors suggested that normalization may have compensated for ASL errors in estimation of the longitudinal magnetization (M_0), and thus improved the consistency between ASL and PET. The above studies suggest that ASL provides robust relative CBF measurements compared with the PET reference standard.

While there remains debate over the value of absolute CBF in clinical evaluation, this controversy may underscore the unavailability and complexity of CBF quantification. Some investigations have identified a CBF threshold (12.7 ml/100 g/min) above which tissue does not infarct in stroke patients⁸⁰; and have identified different CBF thresholds for tissue viability in gray and white matter.⁸³ On the other hand, a recent meta-analysis found high variability in optimal CBF thresholds reported for stroke, from 14.1 to 35.0 ml/100 g/min for penumbra, and from 4.8 to 8.4 ml/100 g/min for the infarct core.⁸⁴ The authors of this meta-analysis highlighted a lack of available quantitative studies, and large heterogeneity between the cohorts and study design. As we gain more experience with ASL, it may be that ASL will generate own reference CBF values that are slightly different from PET. Normalization

methods also remove true differences in absolute CBF between populations. This normalization may pose challenges to CBF comparisons between cohorts, especially in neurodegenerative disorders that may present with early global or diffuse reductions in absolute CBF. Future studies that compare absolute CBF between modalities should focus on the clinical impact of each perfusion imaging technique.

Reproducibility of [^{15}O]-water PET and ASL MRI

Knowledge about the reliability of CBF values over time (intra-subject reproducibility) is critical to accurate interpretation of longitudinal studies in normal brain development, neurodegenerative diseases, and therapeutic interventions. We also need to understand the normal CBF range across subjects (inter-subject reproducibility) to see if differences between patient groups reflect true disease-related changes or simply reflect normal population variations. Previous scan-rescan studies have assessed the repeatability of CBF measured by [^{15}O]-water PET within the same session,^{85–87} or on separate days.^{48,88} Similar ASL studies investigated CBF reproducibility within the same session^{37,89,90} or in scans up to several weeks apart.^{91–95} Because ASL does not require ionizing radiation, repeat ASL scans have also been performed in the same subjects at different time

intervals, ranging from the same session to scans a month apart.^{37,49,96}

CBF reproducibility is affected not only by normal physiological and functional fluctuations in perfusion but also by technical aspects of the imaging modality. For instance, tissue magnetization transfer effects contribute signal fluctuations to pulsed ASL measurements;⁸⁹ transient magnetic fields such as eddy currents also create fluctuations in ASL scans. On the other hand, arterial blood sampling poses a technical source of variability to PET-based CBF maps. To achieve a desired reproducibility of 5% in the AIF, and thus more reliable CBF values, Lebrun-Grandie et al. identified and removed spurious values from the arterial samples that may have reflected timing errors or changes in respiration due to stress from the arterial puncture.⁹⁷

The coefficient of variation (COV, %) for scan-rescan reproducibility (Figure 6(a)) and inter-subject variations in CBF (Figure 6(b)) is summarized across several CBF studies. These COV values include studies that performed only ASL, only PET, or both modalities. In Figure 6(a), the reproducibility was typically determined within same imaging session, except for one study in which ASL scans were separated by up to 4 weeks.¹⁷ As expected, CBF variations between subjects ($\text{COV}_{\text{ASL}} = 14.6\%$ and $\text{COV}_{\text{PET}} = 13.3\%$) were larger than the scan-rescan reproducibility of the measurements ($\text{COV}_{\text{ASL}} = 8.6\%$ and $\text{COV}_{\text{PET}} = 10.1\%$). In the four studies that reported scan-rescan COV for both

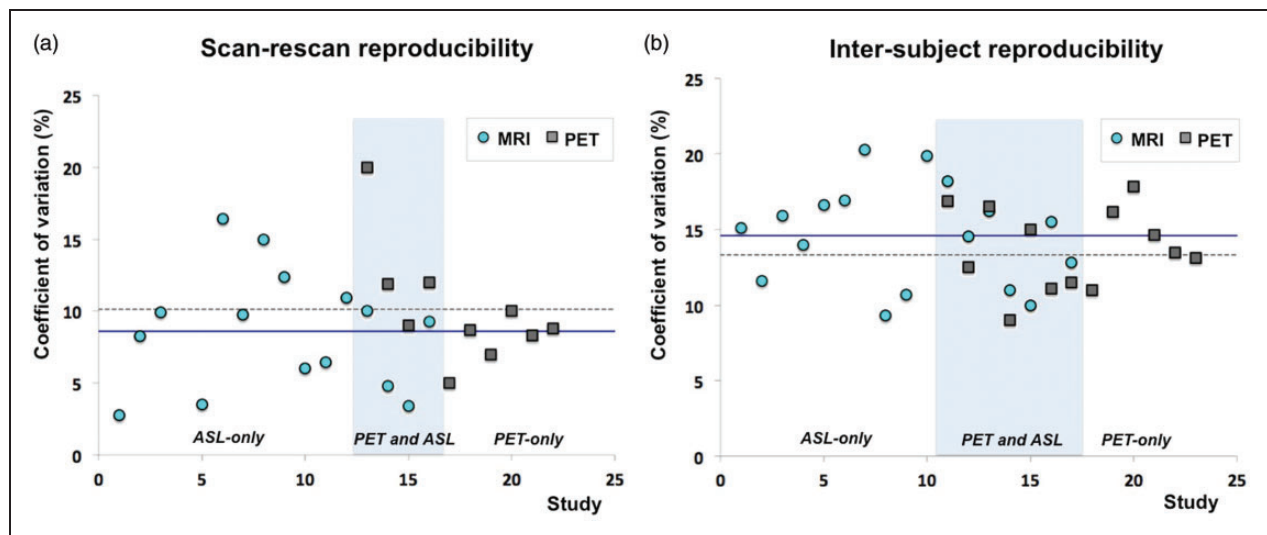


Figure 6. The COV (%) for (a) scan-rescan reproducibility and (b) and between-subject variations in healthy volunteers across CBF studies. The COV values are shown for studies that performed only ASL, only PET, or both modalities (center). Scan-rescan reproducibility was typically determined from the same imaging session, except in one study in which ASL scans were separated by up to 4 weeks. The solid blue lines represent the mean COV for MRI measurements, whereas the dotted gray lines represent the mean COV for PET measurements across the studies. References for each numbered study are presented in Appendix I. COV: coefficient of variation; ASL: arterial spin labeling; MRI: magnetic resonance imaging; PET: positron emission tomography; CBF: cerebral blood flow.

PET and MRI (Figure 6(a)), the scan–rescan reproducibility was consistently better with ASL compared with PET. This observation suggests that ASL may be a suitable replacement for PET in terms of reproducibility.

CBF measurements may also vary across imaging centers, as previously evaluated by multi-site studies of ASL^{35,98,99} and PET.¹⁰⁰ In this review article, the quantitative CBF values in Figure 2 all derive from healthy adults. For the PET reference standard, mean brain CBF values for four of the highlighted studies fell within a tight range of 39–43 ml/100 g/min.^{11,19,23} However, even within the healthy population, Ye et al. measured a higher PET CBF value of 59 ml/100 g/min¹⁴ and van Golen et al. measured a lower PET CBF value of 31 ml/100 g/min.¹² These variations may reflect differences in acquisition methodology, image reconstruction, and analysis across sites that are only recently being explored.^{99,101}

While Figure 6 depicts CBF reproducibility in healthy volunteers, few studies have assessed reproducibility in patient populations. Perfusion status may be more instable in patients due to physiological fluctuations related to pathology and technical artifacts. However, repeat scans are challenging in patients, and the underlying pathology may lead to rapid CBF changes. Kilroy et al. performed both PET and ASL CBF scans in elderly adults including patients with dementia¹⁷ but repeat scans were only available for ASL, likely because ASL studies are technically less challenging than PET. Understanding the scan–rescan COV in patients is important to tailor imaging parameters to the desired longitudinal follow-up and expected magnitude of disease-related CBF changes.

Considerations for future comparison studies

By summarizing studies that performed both ASL MRI and [¹⁵O]-water PET CBF imaging, we identified unmet needs that motivate future comparison studies. In clinical use, ASL is preferred because it does not use ionizing radiation, is relatively simple to set up, and has better scan–rescan reproducibility than PET. ASL also has significant advantages over other MRI techniques such as dynamic susceptibility contrast, which requires injection of a contrast agent and does not provide quantitative CBF values in routine practice. However, in order for ASL to be considered the new standard for CBF imaging, the following shortcomings must be addressed:

A standardized protocol for ASL should be adopted and refined

The acquisition parameters and assumed constants for CBF quantification differed between ASL studies.

For instance, a wide range of assumed T₁ relaxation values in arterial blood (Table 2), and of PLD times may have contributed to variations in ASL CBF across studies (Figure 2). There has been a recent effort to standardize the method, resulting in a consensus protocol for both pulsed and pseudo-continuous ASL.³⁹ This consensus protocol recommends different timing parameters to image various populations, with shorter PLD for children (1500 ms) and longer PLD (2000 ms) for elderly persons over 70 years of age and adult patients. However, the protocol also by necessity utilizes several simplifications, such as a one-compartment model that does not account for tissue T₁ relaxation, to enable wider use of quantitative ASL. We acknowledge that with vast variations in ATT across populations, it is unlikely that a single standard protocol is optimal for all conditions. Nonetheless, it is critical to have a standardized set of parameters that reflect our current understanding of the ASL technique and may be revised as new ASL developments are tested.

Further evaluation of multi-delay ASL is needed in patient populations

Previous PET and MRI comparisons of CBF have mainly focused on healthy volunteers, and there is a lack of studies in patient populations (e.g. with cerebrovascular disease) where standard ASL strategies may fail.²⁰ In clinical settings, CBF maps must be acquired efficiently, and it is usually not possible to acquire “pre-scans” that may help optimize the ASL parameters for individual patients. To achieve sufficient SNR, many multi-delay ASL scans approaches require longer duration scans, which can in turn lead to issues with patient motion in challenging populations. Furthermore, there is limited information about the reproducibility of ASL in patients, which may exhibit higher measurement variance in regions of low flow. MRI perfusion quantification is an established need in imaging of acute ischemic stroke patients, and typically must be performed within hours of symptom onset. Improvement of SNR and reproducibility of ASL in acute stroke would represent a key step forward in the stroke community, especially in the context of imaging to select patients for new endovascular treatments.¹⁰²

Not only must we better understand clinical situations in which standard ASL fails, advanced multi-delay ASL strategies^{18,21,34,62} hold promise in patient populations and should be carefully evaluated against PET in these cohorts. Unfortunately, there is currently no recommended protocol for multi-delay ASL and its successful implementation must overcome several technical challenges. These obstacles include lower SNR due to small flip angles in Look-Locker approaches,^{21,103} the tradeoff between long acquisition

time and poor resolution with sequential acquisitions, and lower CBF reproducibility.¹⁰⁴ Sequential multi-delay ASL approaches typically limit the number of averages and/or spatial resolution to maintain reasonable scan time. Furthermore, the SNR of images at longer PLDs are significantly lower than single-delay ASL acquisitions with the same PLD.

More efficient encoding strategies (e.g. Hadamard encoding¹⁰⁴ and time-encoded pcASL¹⁰⁵), in which labeling blocks are divided up to avoid idle time in sequential PLDs, may improve the SNR of these scans. If a reliable multi-delay ASL is established, this approach may prove ideal for imaging in patients where the ATT is unknown. Other advanced strategies, such as velocity-selective ASL, which labels arterial blood spins based on their flow velocity rather than spatial location, have also begun to show good voxel-wise correlation with [¹⁵O]-water PET and may improve perfusion estimates in challenging patient cases.¹⁰⁶

Multiple CBF observations in different brain states are necessary to map cerebrovascular reserve (CVR)

CVR is the perfusion response of the cerebral vasculature to a “brain stress test” that increases blood flow to the brain (i.e. via a pharmacologic intervention or a breathing challenge). There is increasing interest in clinical CVR measurements, since impaired CVR is a strong predictor of increased risk for ischemic events in patients with steno-occlusive disease independently of baseline CBF values.^{107,108} Because the calculation of CVR maps requires multiple CBF observations, ASL is an ideal imaging tool because of its noninvasive nature. Only one comparison study to date has directly compared CVR maps by both modalities,¹³ and this work found excellent correspondence between PET and ASL for mean CVR values and on a voxel-wise basis. Future studies could further compare CVR by PET and MRI, and evaluate CBF reproducibility across a larger range of different brain states.¹⁰⁹

Hybrid systems can offer simultaneous CBF exams by PET and MRI

Normal physiological CBF fluctuations complicate the agreement between PET and MRI values from separate scan sessions. Not surprisingly, studies in which PET and MRI were closely spaced in time had better agreement (Figure 4). The introduction of PET-MRI systems allows for an ideal validation tool to achieve simultaneous perfusion scans by both modalities and avoid undesired physiological fluctuations.^{11,23} Concurrent high-resolution MRI also allows clear delineation of major arteries to derive an image-based AIF²³ that may better represent tracer delivery at the brain than AIFs

measured from the radial artery in typical PET studies. Although technical challenges such as attenuation correction remain, PET-MRI scanner offers a promising new way to validate ASL against PET in future studies.

Conclusion

The ability to measure CBF in the brain will bring critical benefits in clinical evaluation of cerebrovascular disease, aging and development, and neurodegenerative disorders. Perfusion studies that have compared ASL MRI and [¹⁵O]-water PET reveal the promise of ASL for accurate and reproducible CBF measurements, but vary in ASL methodology and lack sufficient testing in patient populations. Future studies could take advantage of PET-MRI systems for simultaneous CBF validation of newly standardized ASL protocols. Once ASL is validated, clinicians will gain a noninvasive, robust and repeatable imaging method with lower coefficient of variation to investigate quantitative perfusion in the brain.

Funding

The author(s) disclosed receipt of the following financial support for the research, authorship, and/or publication of this article: Stanford Neurosciences Institute Interdisciplinary Scholar Award and GE Healthcare

Acknowledgments

We thank Dr. Jarrett Rosenberg for insightful discussion on data analysis, statistics, and presentation.

Declaration of conflicting interests

The author(s) declared the following potential conflicts of interest with respect to the research, authorship, and/or publication of this article: Dr. Fan receives research support from the Stanford Neurosciences Institute Interdisciplinary Scholar Award and GE Healthcare. Dr. Jahanian receives research support from GE Healthcare. Dr. Holdsworth receives research support from GE Healthcare. Dr. Zaharchuk receives research support from GE Healthcare.

References

1. Wintermark M, Sesay M, Barbier E, et al. Comparative overview of brain perfusion imaging techniques. *J Neuroradiol* 2005; 32: 294–314.
2. Herscovitch P, Markham J and Raichle ME. Brain blood flow measured with intravenous H₂(15)O. I. Theory and error analysis. *J Nucl Med* 1983; 24: 782–789.
3. Raichle ME, Martin WR, Herscovitch P, et al. Brain blood flow measured with intravenous H₂(15)O. II. Implementation and validation. *J Nucl Med* 1983; 24: 790–798.
4. Kety SS and Schmidt CF. The nitrous oxide method for the quantitative determination of cerebral blood flow in man: theory, procedure and normal values. *J Clin Invest* 1948; 27: 476–483.

5. Kwong KK, Chesler DA, Weisskoff RM, et al. MR perfusion studies with T1-weighted echo planar imaging. *Magn Reson Med* 1995; 34: 878–887.
6. Wong EC, Buxton RB and Frank LR. A theoretical and experimental comparison of continuous and pulsed arterial spin labeling techniques for quantitative perfusion imaging. *Magn Reson Med* 1998; 40: 348–355.
7. Kim SG. Quantification of relative cerebral blood flow change by flow-sensitive alternating inversion recovery (FAIR) technique: application to functional mapping. *Magn Reson Med* 1995; 34: 293–301.
8. Detre JA, Leigh JS, Williams DS, et al. Perfusion imaging. *Magn Reson Med* 1992; 23: 37–45.
9. Williams DS, Detre JA, Leigh JS, et al. Magnetic resonance imaging of perfusion using spin inversion of arterial water. *Proc Natl Acad Sci USA* 1992; 89: 212–216.
10. Dai W, Garcia D, de Bazelaire C, et al. Continuous flow-driven inversion for arterial spin labeling using pulsed radio frequency and gradient fields. *Magn Reson Med* 2008; 60: 1488–1497.
11. Zhang K, Herzog H, Mauler J, et al. Comparison of cerebral blood flow acquired by simultaneous [^{15}O]water positron emission tomography and arterial spin labeling magnetic resonance imaging. *J Cerebr Blood Flow Metab* 2014; 34: 1373–1380.
12. van Golen LW, Kuijter JP, Huisman MC, et al. Quantification of cerebral blood flow in healthy volunteers and type 1 diabetic patients: comparison of MRI arterial spin labeling and [(15)O]H₂O positron emission tomography (PET). *J Magn Reson Imaging* 2014; 40: 1300–1309.
13. Heijtel DF, Mutsaerts HJ, Bakker E, et al. Accuracy and precision of pseudo-continuous arterial spin labeling perfusion during baseline and hypercapnia: a head-to-head comparison with (1)(5)O H(2)O positron emission tomography. *NeuroImage Clin* 2014; 92: 182–192.
14. Ye FQ, Berman KF, Ellmore T, et al. H(2)(15)O PET validation of steady-state arterial spin tagging cerebral blood flow measurements in humans. *Magn Reson Med* 2000; 44: 450–456.
15. Qiu M, Paul Maguire R, Arora J, et al. Arterial transit time effects in pulsed arterial spin labeling CBF mapping: insight from a PET and MR study in normal human subjects. *Magn Reson Med* 2010; 63: 374–384.
16. Xu G, Rowley HA, Wu G, et al. Reliability and precision of pseudo-continuous arterial spin labeling perfusion MRI on 3.0 T and comparison with 15O-water PET in elderly subjects at risk for Alzheimer's disease. *NMR Biomed* 2010; 23: 286–293.
17. Kilroy E, Apostolova L, Liu C, et al. Reliability of two-dimensional and three-dimensional pseudo-continuous arterial spin labeling perfusion MRI in elderly populations: comparison with 15O-water positron emission tomography. *J Magn Reson Imaging* 2014; 39: 931–939.
18. Kamano H, Yoshiura T, Hiwatashi A, et al. Arterial spin labeling in patients with chronic cerebral artery stenocclusive disease: correlation with (15)O-PET. *Acta Radiol* 2013; 54: 99–106.
19. Henriksen OM, Larsson HB, Hansen AE, et al. Estimation of intersubject variability of cerebral blood flow measurements using MRI and positron emission tomography. *J Magn Reson Imaging* 2012; 35: 1290–1299.
20. Goetti R, Warnock G, Kuhn FP, et al. Quantitative cerebral perfusion imaging in children and young adults with Moyamoya disease: comparison of arterial spin-labeling-MRI and H(2)(15)O-PET. *AJNR American J Neuroradiol* 2014; 35: 1022–1028.
21. Bokkers RP, Bremmer JP, van Berckel BN, et al. Arterial spin labeling perfusion MRI at multiple delay times: a correlative study with H(2)(15)O positron emission tomography in patients with symptomatic carotid artery occlusion. *J Cerebr Blood Flow Metab* 2010; 30: 222–229.
22. Boellaard R, Knaapen P, Rijbroek A, et al. Evaluation of basis function and linear least squares methods for generating parametric blood flow images using 15O-water and Positron Emission Tomography. *Mol Imag Biol* 2005; 7: 273–285.
23. Su Y, Vlassenko A, Blazey T, et al. Comparison of cerebral blood flow measurement obtained from simultaneously acquired ASL and O15-water PET. *J Nucl Med* 2014; 55(Supplement 1): 207.
24. Petersen ET, Lim T and Golay X. Model-free arterial spin labeling quantification approach for perfusion MRI. *Magn Reson Med* 2006; 55: 219–232.
25. Wu WC, St Lawrence KS, Licht DJ, et al. Quantification issues in arterial spin labeling perfusion magnetic resonance imaging. *Top Magn Reson Imag* 2010; 21: 65–73.
26. Jahanian H, Peltier S, Noll DC, et al. Arterial cerebral blood volume-weighted functional MRI using pseudo-continuous arterial spin tagging (AVAST). *Magn Reson Med* 2015; 73: 1053–1064.
27. De Vis JB, Hendrikse J, Groenendaal F, et al. Impact of neonate haematocrit variability on the longitudinal relaxation time of blood: Implications for arterial spin labeling MRI. *NeuroImage Clin* 2014; 4: 517–525.
28. Parkes LM and Tofts PS. Improved accuracy of human cerebral blood perfusion measurements using arterial spin labeling: accounting for capillary water permeability. *Magn Reson Med* 2002; 48: 27–41.
29. Steen RG, Gronemeyer SA, Kingsley PB, et al. Precise and accurate measurement of proton T1 in human brain in vivo: validation and preliminary clinical application. *J Magn Reson Imaging* 1994; 4: 681–691.
30. Lu H, Clingman C, Golay X, et al. Determining the longitudinal relaxation time (T1) of blood at 3.0 Tesla. *Magn Reson Med* 2004; 52: 679–682.
31. Jahanian H, Noll DC and Hernandez-Garcia L. B0 field inhomogeneity considerations in pseudo-continuous arterial spin labeling (pCASL): effects on tagging efficiency and correction strategy. *NMR Biomed* 2011; 24: 1202–1209.
32. Aslan S, Xu F, Wang PL, et al. Estimation of labeling efficiency in pseudocontinuous arterial spin labeling. *Magn Reson Med* 2010; 63: 765–771.
33. Zhang J. How far is arterial spin labeling MRI from a clinical reality? Insights from arterial spin labeling comparative studies in Alzheimer's disease and other neurological disorders. *J Magn Reson Imaging* 2015. DOI: 10.1002/jmri.25022.

34. Qiu D, Straka M, Zun Z, et al. CBF measurements using multidelay pseudocontinuous and velocity-selective arterial spin labeling in patients with long arterial transit delays: comparison with xenon CT CBF. *J Magn Reson Imaging* 2012; 36: 110–119.
35. Gevers S, van Osch MJ, Bokkers RP, et al. Intra- and multicenter reproducibility of pulsed, continuous and pseudo-continuous arterial spin labeling methods for measuring cerebral perfusion. *J Cerebr Blood Flow Metab* 2011; 31: 1706–1715.
36. Tancredi FB, Gauthier CJ, Madjar C, et al. Comparison of pulsed and pseudocontinuous arterial spin-labeling for measuring CO₂-induced cerebrovascular reactivity. *J Magn Reson Imaging* 2012; 36: 312–321.
37. Chen Y, Wang DJ and Detre JA. Test-retest reliability of arterial spin labeling with common labeling strategies. *J Magn Reson Imaging* 2011; 33: 940–949.
38. Donahue MJ, Lu H, Jones CK, et al. An account of the discrepancy between MRI and PET cerebral blood flow measures. A high-field MRI investigation. *NMR Biomed* 2006; 19: 1043–1054.
39. Alsop DC, Detre JA, Golay X, et al. Recommended implementation of arterial spin-labeled perfusion MRI for clinical applications: A consensus of the ISMRM perfusion study group and the European consortium for ASL in dementia. *Magn Reson Med* 2015; 73: 102–116.
40. van Osch MJ, Teeuwisse WM, van Walderveen MA, et al. Can arterial spin labeling detect white matter perfusion signal? *Magn Reson Med* 2009; 62: 165–173.
41. van Gelderen P, de Zwart JA and Duyn JH. Pitfalls of MRI measurement of white matter perfusion based on arterial spin labeling. *Magn Reson Med* 2008; 59: 788–795.
42. Ashburner J and Friston KJ. Voxel-based morphometry—the methods. *NeuroImage* 2000; 11(6 Pt 1): 805–821.
43. Meltzer CC, Cantwell MN, Greer PJ, et al. Does cerebral blood flow decline in healthy aging? A PET study with partial-volume correction. *J Nucl Med* 2000; 41: 1842–1848.
44. Iida H, Law I, Pakkenberg B, et al. Quantitation of regional cerebral blood flow corrected for partial volume effect using O-15 water and PET: I. Theory, error analysis, and stereologic comparison. *J Cerebr Blood Flow Metab* 2000; 20: 1237–1251.
45. Law I, Iida H, Holm S, et al. Quantitation of regional cerebral blood flow corrected for partial volume effect using O-15 water and PET: II. Normal values and gray matter blood flow response to visual activation. *J Cerebr Blood Flow Metab* 2000; 20: 1252–1263.
46. Asllani I, Borogovac A and Brown TR. Regression algorithm correcting for partial volume effects in arterial spin labeling MRI. *Magn Reson Med* 2008; 60: 1362–1371.
47. Chappell MA, Groves AR, MacIntosh BJ, et al. Partial volume correction of multiple inversion time arterial spin labeling MRI data. *Magn Reson Med* 2011; 65: 1173–1183.
48. Carroll TJ, Teneggi V, Jobin M, et al. Absolute quantification of cerebral blood flow with magnetic resonance, reproducibility of the method, and comparison with H₂(15)O positron emission tomography. *J Cerebr Blood Flow Metab* 2002; 22: 1149–1156.
49. Floyd TF, Ratcliffe SJ, Wang J, et al. Precision of the CASL-perfusion MRI technique for the measurement of cerebral blood flow in whole brain and vascular territories. *J Magn Reson Imaging* 2003; 18: 649–655.
50. Conroy DA, Spielman AJ and Scott RQ. Daily rhythm of cerebral blood flow velocity. *J Circadian Rhythms* 2005; 3(0), p.Art. 3. DOI: <http://doi.org/10.1186/1740-3391-3-3>.
51. Wauschkuhn CA, Witte K, Gorbey S, et al. Circadian periodicity of cerebral blood flow revealed by laser-Doppler flowmetry in awake rats: relation to blood pressure and activity. *Am J Physiol Heart Circ Physiol* 2005; 289: H1662–H1668.
52. Cosgrove KP, Mazure CM and Staley JK. Evolving knowledge of sex differences in brain structure, function, and chemistry. *Biol Psychiatry* 2007; 62: 847–855.
53. Field AS, Laurienti PJ, Yen YF, et al. Dietary caffeine consumption and withdrawal: confounding variables in quantitative cerebral perfusion studies? *Radiology* 2003; 227: 129–135.
54. Mathew RJ and Wilson WH. Caffeine induced changes in cerebral circulation. *Stroke* 1985; 16: 814–817.
55. Marchal G, Rioux P, Petit-Taboue MC, et al. Regional cerebral oxygen consumption, blood flow, and blood volume in healthy human aging. *Archiv Neurol* 1992; 49: 1013–1020.
56. Bartenstein P, Minoshima S, Hirsch C, et al. Quantitative assessment of cerebral blood flow in patients with Alzheimer's disease by SPECT. *J Nucl Med* 1997; 38: 1095–1101.
57. Matsuda H. Cerebral blood flow and metabolic abnormalities in Alzheimer's disease. *Ann Nucl Med* 2001; 15: 85–92.
58. Yamauchi H, Fukuyama H, Nagahama Y, et al. Evidence of misery perfusion and risk for recurrent stroke in major cerebral arterial occlusive diseases from PET. *J Neurol Neurosurg Psychiatry* 1996; 61: 18–25.
59. Powers WJ. Cerebral hemodynamics in ischemic cerebrovascular disease. *Ann Neurol* 1991; 29: 231–240.
60. Lin W, Celik A, Derdeyn C, et al. Quantitative measurements of cerebral blood flow in patients with unilateral carotid artery occlusion: a PET and MR study. *J Magn Reson Imaging* 2001; 14: 659–667.
61. Liebeskind DS. Collateral circulation. *Stroke* 2003; 34: 2279–2284.
62. Martin SZ, Madai VI, von Samson-Himmelstjerna FC, et al. 3D GRASE pulsed arterial spin labeling at multiple inflow times in patients with long arterial transit times: comparison with dynamic susceptibility-weighted contrast-enhanced MRI at 3 Tesla. *J Cerebr Blood Flow Metab* 2015; 35: 392–401.
63. Buxton RB, Frank LR, Wong EC, et al. A general kinetic model for quantitative perfusion imaging with arterial spin labeling. *Magn Reson Med* 1998; 40: 383–396.
64. Pantano P, Baron JC, Lebrun-Grandie P, et al. Regional cerebral blood flow and oxygen consumption in human aging. *Stroke* 1984; 15: 635–641.

65. Liu Y, Zhu X, Feinberg D, et al. Arterial spin labeling MRI study of age and gender effects on brain perfusion hemodynamics. *Magn Reson Med* 2012; 68: 912–922.
66. Itoh M, Hatazawa J, Miyazawa H, et al. Stability of cerebral blood flow and oxygen metabolism during normal aging. *Gerontology* 1990; 36: 43–48.
67. Xu G, Antuono PG, Jones J, et al. Perfusion fMRI detects deficits in regional CBF during memory-encoding tasks in MCI subjects. *Neurology* 2007; 69: 1650–1656.
68. Alsop DC, Detre JA and Grossman M. Assessment of cerebral blood flow in Alzheimer's disease by spin-labeled magnetic resonance imaging. *Ann Neurol* 2000; 47: 93–100.
69. Johnson NA, Jahng GH, Weiner MW, et al. Pattern of cerebral hypoperfusion in Alzheimer disease and mild cognitive impairment measured with arterial spin-labeling MR imaging: initial experience. *Radiology* 2005; 234: 851–859.
70. Campbell AM and Beaulieu C. Pulsed arterial spin labeling parameter optimization for an elderly population. *J Magn Reson Imaging* 2006; 23: 398–403.
71. Mah E and Bruno RS. Postprandial hyperglycemia on vascular endothelial function: mechanisms and consequences. *Nutr Res* 2012; 32: 727–740.
72. Quirce R, Carril JM, Jimenez-Bonilla JF, et al. Semi-quantitative assessment of cerebral blood flow with 99mTc-HMPAO SPET in type I diabetic patients with no clinical history of cerebrovascular disease. *Eur J Nucl Med* 1997; 24: 1507–1513.
73. Salem MA, Matta LF, Tantawy AA, et al. Single photon emission tomography (SPECT) study of regional cerebral blood flow in normoalbuminuric children and adolescents with type I diabetes. *Pediatr Diab* 2002; 3: 155–162.
74. Schwartz WJ, Smith CB, Davidsen L, et al. Metabolic mapping of functional activity in the hypothalamo-neurohypophysial system of the rat. *Science* 1979; 205: 723–725.
75. Powers WJ, Hirsch IB and Cryer PE. Effect of stepped hypoglycemia on regional cerebral blood flow response to physiological brain activation. *Am J Physiol* 1996; 270(2 Pt 2): H554–H559.
76. Teves D, Videen TO, Cryer PE, et al. Activation of human medial prefrontal cortex during autonomic responses to hypoglycemia. *Proc Natl Acad Sci USA* 2004; 101: 6217–6221.
77. Arbelaez AM, Powers WJ, Videen TO, et al. Attenuation of counterregulatory responses to recurrent hypoglycemia by active thalamic inhibition: a mechanism for hypoglycemia-associated autonomic failure. *Diabetes* 2008; 57: 470–475.
78. Grandin CB, Duprez TP, Smith AM, et al. Which MR-derived perfusion parameters are the best predictors of infarct growth in hyperacute stroke? Comparative study between relative and quantitative measurements. *Radiology* 2002; 223: 361–370.
79. Lev MH, Gonzalez RG, Schaefer PW, et al. Cerebral blood flow thresholds in acute stroke triage. *Stroke* 2006; 37: 2202. author reply 2203.
80. Schaefer PW, Roccatagliata L, Ledezma C, et al. First-pass quantitative CT perfusion identifies thresholds for salvageable penumbra in acute stroke patients treated with intra-arterial therapy. *AJNR Am J Neuroradiol* 2006; 27: 20–25.
81. Chen JJ, Wieckowska M, Meyer E, et al. Cerebral blood flow measurement using fMRI and PET: a cross-validation study. *Int J Biomed Imag* 2008; 2008: 516359.
82. Feng CM, Narayana S, Lancaster JL, et al. CBF changes during brain activation: fMRI vs. PET. *NeuroImage* 2004; 22: 443–446.
83. Bristow MS, Simon JE, Brown RA, et al. MR perfusion and diffusion in acute ischemic stroke: human gray and white matter have different thresholds for infarction. *J Cerebr Blood Flow Metab* 2005; 25: 1280–1287.
84. Bandera E, Botteri M, Minelli C, et al. Cerebral blood flow threshold of ischemic penumbra and infarct core in acute ischemic stroke: a systematic review. *Stroke* 2006; 37: 1334–1339.
85. Frackowiak RS, Jones T, Lenzi GL, et al. Regional cerebral oxygen utilization and blood flow in normal man using oxygen-15 and positron emission tomography. *Acta Neurol Scand* 1980; 62: 336–344.
86. Matthew E, Andreason P, Carson RE, et al. Reproducibility of resting cerebral blood flow measurements with H2(15)O positron emission tomography in humans. *J Cerebr Blood Flow Metab* 1993; 13: 748–754.
87. Coles JP, Fryer TD, Bradley PG, et al. Intersubject variability and reproducibility of 15O PET studies. *J Cerebr Blood Flow Metab* 2006; 26: 48–57.
88. Bremner JP, van Berckel BN, Persoon S, et al. Day-to-day test-retest variability of CBF, CMRO2, and OEF measurements using dynamic 15O PET studies. *Mol Imag Biol* 2011; 13: 759–768.
89. Jahng GH, Song E, Zhu XP, et al. Human brain: reliability and reproducibility of pulsed arterial spin-labeling perfusion MR imaging. *Radiology* 2005; 234: 909–916.
90. Parkes LM, Rashid W, Chard DT, et al. Normal cerebral perfusion measurements using arterial spin labeling: reproducibility, stability, and age and gender effects. *Magn Reson Med* 2004; 51: 736–743.
91. Hermes M, Hagemann D, Britz P, et al. Reproducibility of continuous arterial spin labeling perfusion MRI after 7 weeks. *Magma* 2007; 20: 103–115.
92. Wang Y, Saykin AJ, Pfeuffer J, et al. Regional reproducibility of pulsed arterial spin labeling perfusion imaging at 3T. *NeuroImage* 2011; 54: 1188–1195.
93. Jain V, Duda J, Avants B, et al. Longitudinal reproducibility and accuracy of pseudo-continuous arterial spin-labeled perfusion MR imaging in typically developing children. *Radiology* 2012; 263: 527–536.
94. Tatewaki Y, Higano S, Taki Y, et al. Regional reliability of quantitative signal targeting with alternating radiofrequency (STAR) labeling of arterial regions (QUASAR). *J Neuroimag* 2014; 24: 554–561.
95. Wu B, Lou X, Wu X, et al. Intra- and interscanner reliability and reproducibility of 3D whole-brain pseudo-continuous arterial spin-labeling MR perfusion at 3T. *J Magn Reson Imaging* 2014; 39: 402–409.
96. Mezue M, Segerdahl AR, Okell TW, et al. Optimization and reliability of multiple postlabeling delay pseudo-continuous arterial spin labeling during rest and

- stimulus-induced functional task activation. *J Cerebr Blood Flow Metab* 2014; 34: 1919–1927.
97. Lebrun-Grandie P, Baron JC, Soussaline F, et al. Coupling between regional blood flow and oxygen utilization in the normal human brain. A study with positron tomography and oxygen 15. *Archiv Neurol* 1983; 40: 230–236.
 98. Petersen ET, Mouridsen K, Golay X, et al. The QUASAR reproducibility study, Part II: Results from a multi-center Arterial Spin Labeling test-retest study. *NeuroImage* 2010; 49: 104–113.
 99. Mutsaerts HJ, van Osch MJ, Zelaya FO, et al. Multi-vendor reliability of arterial spin labeling perfusion MRI using a near-identical sequence: Implications for multi-center studies. *NeuroImage* 2015; 113: 143–152.
 100. Ito H, Kanno I, Kato C, et al. Database of normal human cerebral blood flow, cerebral blood volume, cerebral oxygen extraction fraction and cerebral metabolic rate of oxygen measured by positron emission tomography with ^{15}O -labelled carbon dioxide or water, carbon monoxide and oxygen: a multicentre study in Japan. *Eur J Nucl Med Mol Imag* 2004; 31: 635–643.
 101. Steketee RM, Mutsaerts HJ, Bron EE, et al. Quantitative functional arterial spin labeling (fASL) MRI—sensitivity and reproducibility of regional CBF changes using pseudo-continuous ASL product sequences. *PloS One* 2015; 10: e0132929.
 102. Menon BK, Campbell BC, Levi C, et al. Role of imaging in current acute ischemic stroke workflow for endovascular therapy. *Stroke* 2015; 46: 1453–1461.
 103. Gunther M, Bock M and Schad LR. Arterial spin labeling in combination with a look-locker sampling strategy: inflow turbo-sampling EPI-FAIR (ITS-FAIR). *Magn Reson Med* 2001; 46: 974–984.
 104. Dai W, Shankaranarayanan A and Alsop DC. Volumetric measurement of perfusion and arterial transit delay using hadamard encoded continuous arterial spin labeling. *Magn Reson Med* 2013; 69: 1014–1022.
 105. Teeuwisse WM, Schmid S, Ghariq E, et al. Time-encoded pseudocontinuous arterial spin labeling: basic properties and timing strategies for human applications. *Magn Reson Med* 2014; 72: 1712–1722.
 106. Schmid S, Heijtel DF, Mutsaerts HJ, et al. Comparison of velocity- and acceleration-selective arterial spin labeling with ^{15}O H $_2\text{O}$ positron emission tomography. *J Cerebr Blood Flow Metab* 2015; 35: 1296–1303.
 107. Gupta A, Chazen JL, Hartman M, et al. Cerebrovascular reserve and stroke risk in patients with carotid stenosis or occlusion: a systematic review and meta-analysis. *Stroke* 2012; 43: 2884–2891.
 108. Reinhard M, Schwarzer G, Briel M, et al. Cerebrovascular reactivity predicts stroke in high-grade carotid artery disease. *Neurology* 2014; 83: 1424–1431.
 109. Yen YF, Field AS, Martin EM, et al. Test-retest reproducibility of quantitative CBF measurements using FAIR perfusion MRI and acetazolamide challenge. *Magn Reson Med* 2002; 47: 921–928.
 110. Frackowiak RS, Lenzi GL, Jones T, et al. Quantitative measurement of regional cerebral blood flow and oxygen metabolism in man using ^{15}O and positron emission tomography: theory, procedure, and normal values. *J Comput Assist Tomogr* 1980; 4: 727–736.

Appendix I

References for coefficients of variation in Figure 6

Figure 6(a). Scan-rescan reproducibility.

ASL-only	Studies ^{16,17,89,90,35,37,92–96,98}
PET and ASL	Studies ^{13,15,19,23}
PET-only	Studies ^{14,48,86–88,110}

Figure 6(b). Inter-subject reproducibility.

ASL-only	Studies ^{16,17,35,37,90,92,93,95,96,98}
PET and ASL	Studies ^{11–15,19,23}
PET-only	Studies ^{43,86–88,100,110}